ISSN 2278-3091
Volume 9, No.5, September - October 2020
International Journal of Advanced Trends in Computer Science and Engineering
Available Online at http://www.warse.org/IJATCSE/static/pdf/file/ijatcse188952020.pdf
https://doi.org/10.30534/ijatcse/2020/188952020

Design and Simulation the Compliant Linear-Rotary Mechanism with Thermal Actuator

Duy Tuan Le[1], Ngoc Dang Khoa Tran[2], Ngoc Tran Le[3]
[1]Faculty of Mechanical Engineering, Industrial University Of Ho Chi Minh City, Ho Chi Minh City, Vietnam, leduytuan@iuh.edu.vn
[2]Faculty of Mechanical Engineering, Industrial University Of Ho Chi Minh City, Ho Chi Minh City, Vietnam, tranngocdangkhoa@iuh.edu.vn
[3]Faculty of Mechanical Engineering, Industrial University Of Ho Chi Minh City, Ho Chi Minh City, Vietnam, Corresponding author : lengoctran@iuh.edu.vn

ABSTRACT

A compliant mechanism to convert linear motion to rotary motion is developed. The means to achieve the linear-to-rotary motion transduction is attributed to an asymmetric arrangement of two linear motion inputs. V-beam thermal actuators provide the linear motion. The device operates with Joule heating effects and the current is applied. Finite element analyses were carried out to predict behaviors of the transduction mechanism. A transduction ratio of nearly 0.5 degrees/mm is achieved. The simulation results also reveal that a more uniform temperature distribution along the thermal actuator allows for a more extended overall thermal expansion and a larger linear motion, which adds to the rotary motion output.

Key words : linear motion, rotation, heat transfer, compliant mechanism.

1. INTRODUCTION

Rotary micro positioners can see applications in hard disk drives [1], positioning stages [2], and micro-manipulators [3]. Lau et al. [1] developed a rotary micro-positioner driven by thermal expansion of silicon/polymer composites. Yi et al. [2] presented a three degree-of-freedom (DOF) micropositioning mechanism with flexural hinges. It requires 12 piezoelectric actuators to achieve two-position DOFs and one angular DOF of their platform. Chao et al. [3] reported a rotary stage with three linear motion input and nine flexural hinges. To achieve high precision, they selected piezoelectric ceramic elements as actuators. Arefin et al. [4] presented a rotary stage actuated by thermal expansion of beam segments. A compact compliant rotational mechanism formed on a double four-bar mechanism is introduced by Zhu et al. [5]. It transfers the linear motion from a piezoelectric actuator into the rotational motion. Wang et al. [6] demonstrated an unreverberation rotary positioner, which works with 4 piezoelectric actuators. The mechanism can work the high velocity. Na et al. [7] proposed a monolithic mechanism that converts the linear movement to rotary motion. The piezo electrical actuator provides the linear motion. However, the mechanism is complex and the limitation in the rotary angle, suitable for the mechanisms, has the tiny rotary angles. A simple device that converts the linear motion into the rotation in out-of-plane is introduced by Wang et al. [8]. The structure combines two disks and flexible beams in a three-dimension model. When the linear displacement applies to the first disk, the flexible beam deforms and makes the second disk rotates. However, this mechanism is hard in fabrication for microdevices. Kothori et al. [9] also described a simple device with rotation and linear motion, but the experiment should be examined to verify the theory.

One of the most popular mechanisms that transform the linear motion into rotational motion is the crank-slider mechanism. A jointless crank slider mechanism is presented by Pardeshi et al. [10]. The structure includes rigid links and the flexure hinges. Dao and Huang [11] investigated the dynamic behavior of a compliant crank-slider. Gupta et al. [12] also analyze the compliant crank-slider mechanism with the encouragement of finite element method.

Electrothermal actuators have many applied for linear motion for micromechanisms. The displacement is supplied by the expansion of a mechanism with current input. V-shaped beams are the popular actuators for in-plane displacement in the microsystem. A study of Chevron actuators is introduced by Chiorean et al. [13]. This study investigates the effectiveness of the design parameter of the mechanism. The finite element method (FEM) is also employed to analyze the V-shaped beam's angle, which Joshi et al. proposed [14]. Simulation with Abaqus software employed in many structure [15]. Baracu et al. [16] designed the Chevron type thermal actuators formed on multiple V beams and fabricated by Reactive Ion Etching (RIE) processing. An improvement of chevron actuators is fabricated based on the multi-user MEMS process (MUMPs), give the mechanism deflects in two directions [17]. Various shapes of V-beam thermal actuators are investigated [18], capable of creating large displacement with the same input current. The V-beam thermal actuators are a suitable mechanism that requires the in-plane linear displacement.

In the study, a combination of V-beam thermal actuator and the linear-rotary mechanism is introduced. The electric current applies in the thermal actuator and the the displacement makes the device rotates. The simulation of the model with Abaqus software assists the analysis to investigate the behavior of the mechanism.

2. DESIGN

Figure 1(a) is a schematic of a linear-to-rotary motion converter. It consists of a rotary stage, two curved beams and two chevron-type electrothermal actuators. The symmetric arrangement of the two actuators facilitates the rotation of the rotary stage. When an electric current, I, is passed through the actuators anchored at its two ends (see Figure 1(b)), thermal expansion caused by Joule heating pushes the apex outward to induce a linear motion in x-axis which makes the rotary stage rotates clockwise with the angle θ. After the current is removed, the two actuators retract and the rotary stage returns to its original orientation (see Figure 1(c)). The dimensions of the device are illustrated in Figure 2. The material parameters used in these simulations are listed in Table 1.

Table 1. Parameters used for the analysis

Parameter	**Value**
Elastic Modulus of silicon (*E*)	130×10^{3} MPa
Poisson's ratio silicon (ν)	0.28
Thermal conductivity ($k_{Si}^{20^oC}$)	1.5494×10^{8} pW/μm.C
Specific resistance ($\rho_0^{20^oC}$)	2.5604×10^{-9} Ω. μm
Co-efficient of thermal expansion of silicon (α)	3.0600×10^{-6} K^{-1}
Thickness of air (t_{air})	1μm

A three-dimension of the device is performed in figure 3; the fabrication employs MEMS technology. So, anchors of the device contact with the substrate and the thermal actuators and rotary components have the substrate gap. The electrical wires connect with electrode pads, provides the current for the thermal actuator.

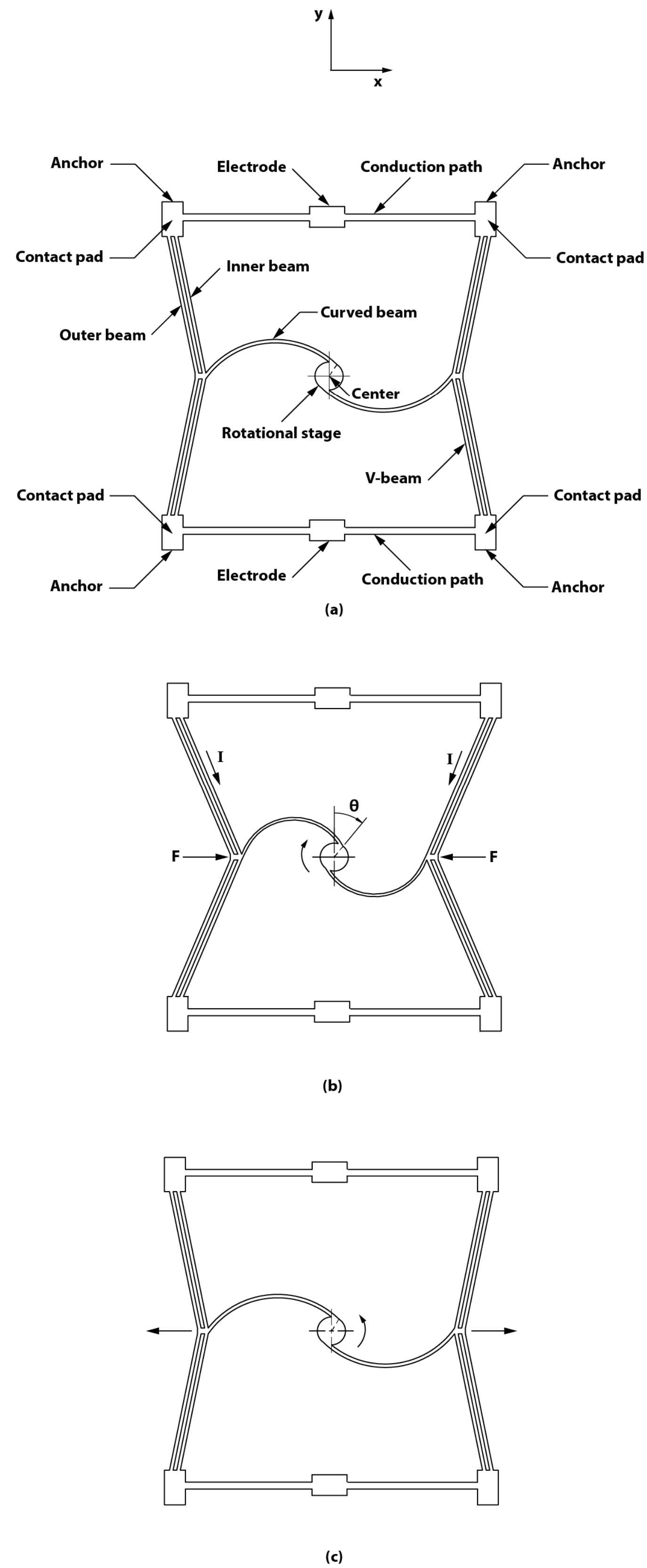

Figure 1: Model of compliant bistable mechanism.

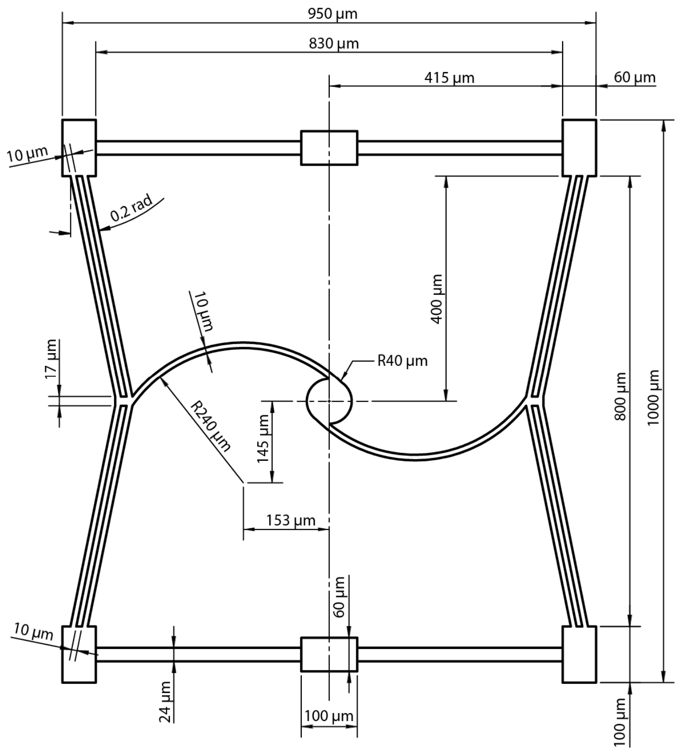

Figure 2: Dimensions of the device.

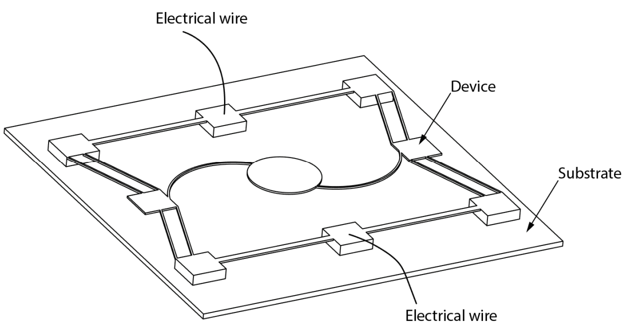

Figure 3: 3D model of the device

3. SIMULATION

In order to obtain the thermal and mechanical behaviors of the device, three-dimensional finite element analyses are carried out. The coupled analyses are divided into two steps. First, electro-thermal analysis is performed to find temperature distribution of the device under current loading. Then, thermal-mechanical analysis is employed to compute the rotation angle of the rotary stage based on the temperature distribution.

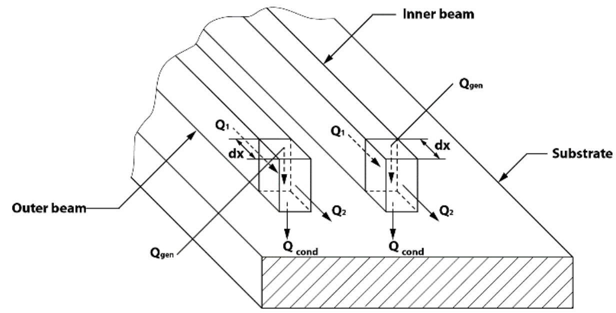

Figure 4: Heat transfer paths involved in an infinitesimal element of an electrothermal actuator.

Due to the size scale of the device, heat loss due to free convection is negligible and is not included in the analyses. The effect of radiation is assumed to be small and could reasonably be ignored. Heat conduction from the device through the surrounding air to the substrate is not negligible and must be accounted for. Figure 4 illustrates the heat transfer paths involved in an infinitesimal element of the electrothermal actuator. In the figure, Q_{gen} is the heat generation due to the applied current. The heat conduction into the element and heat conducted out to the beam are marked as Q_1 and Q_2, respectively. Q_{cond} is the conduction loss through the air gap and into the substrate.

Current is applied between the fixed ends (anchor pads) of the electrothermal actuators. The commercial software, ABAQUS, is employed for the finite element analyses. The material of the device is Silicon, which properties are listed in Table 1. Figure 5 shows a mesh for the model. A mesh sensitivity analysis is performed to assure convergence of the solution.

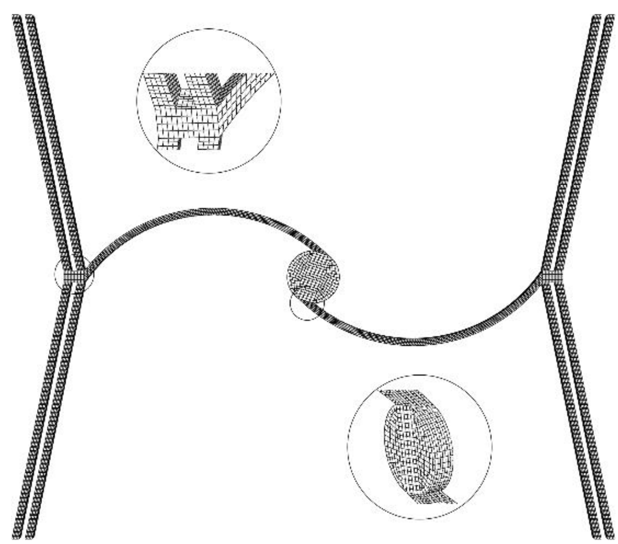

Figure 5: A mesh of the model.

4. ANALYSES

Figure 6 is a plot of the maximum temperature versus applied current. For the current ranging from 0 to 0.1 A, the maximum temperature increases almost linearly as the current increases. The temperature distribution of the device under 0.1 A current loading is shown in Figure 7. The maximum temperature is 847^{o}C, which is well below the typical melting point of silicon, 1400^{o}C. Figure 8 shows the linear displacement of the apex, d, of the electrothermal actuator and the rotation angle of the rotary stage, θ, versus the applied current. Initially, d and θ increase gradually with the increase of current. When the current increases further, rate of increase of d and θ is higher. The transduction ratio, θ /d, is nearly 0.5 degree/μm.

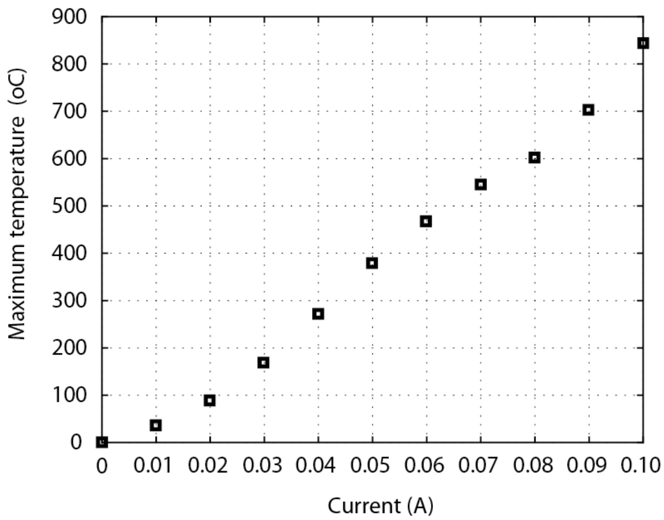

Figure 6: Maximum temperature versus driving current.

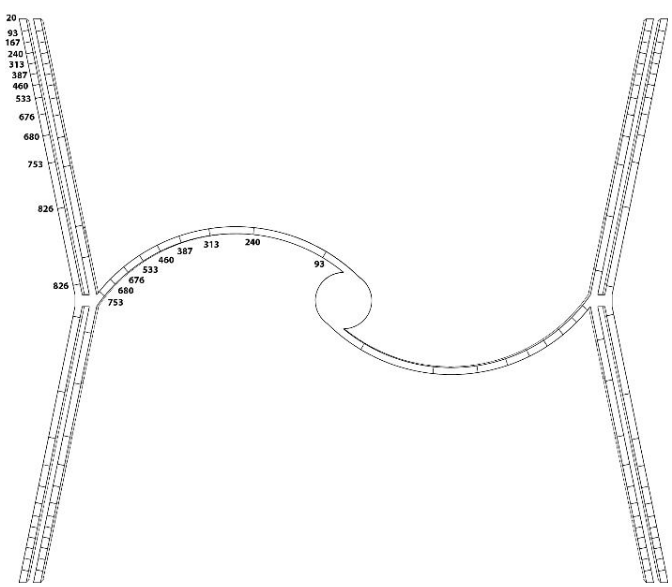

Figure 7: Temperature distribution of the motion converter.

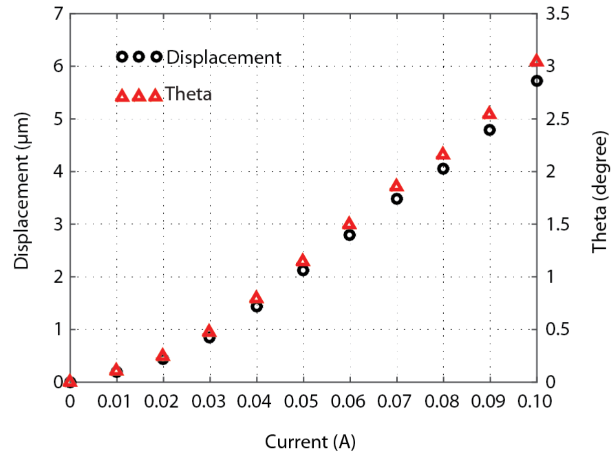

Figure 8: Maximum rotation angle and maximum displacement versus driving current.

In order to avoid plastic deformation, it is necessary to maintain the magnitude of the maximum Mises stress below the yield stress of the material. The maximum Mises stress, 194 Mpa, under the current loading of 0.1 A is well below the typical value of yield stress of silicon, 7 GPa. Performance comparison with published linear-to-rotary motion converter will be carried out to validate the effectiveness of the developed device. Prototypes of the device will be fabricated to examine the device experimentally.

5. CONCLUSION

A design and analysis of a linear-to-rotary motion converter is presented. Base on electro-thermal-mechanical coupled finite element analyses, the device has a transduction ratio of input displacement to output angle of 0.5 degree/μm is obtained under a current loading of 0.1 A. The maximus temperature and maximus Mises stress are well below the typical melting point and yield stress of silicon material.

REFERENCES

1. G. K. Lau, J. Yang, C. P. Tan and N. B. Chong. **An electro-thermally activated rotary micro-positioner for slider-level dual-stage positioning in hard disk drives**, *J. Micromech. Microeng.*, vol. 26, 035016, 2016.
2. B. J. Yi, G. B. Chung, H. Y. Na, W. K. Kim and I. H. Suh. **Design and experiment of a 3-DOF parallel micromechanism utilizing flexure hinges**, *IEEE Transactions on Robotics and Automation*, vol. 19, pp. 604-611, 2003.
3. D. Chao, G., Zong and R. Liu. **Design of a 6-DOF compliant manipulator based on serial-parallel architecture**, *2005 IEEE/ASME International Conference on Advanced Intelligent Mechatronics*, vols. 1 and 2, IEEE (2005), pp. 765–770.

4. M. Arefin, M. Packirisamy and A. K. W. Ahmed. **Disc type thermal actuator with straight beams for angular motion**, *Applied Thermal Engineering*, vol. 51, pp. 988-999, 2013.
5. X. Zhu, Z. Wen, G. Chen, J. Liang and P. Liu. **A decoupled flexure-based rotary micropositioning stage with compact size**, *Proceedings of Institute of Mechanical Engineering, Part C: Journal of Mechanical Engineering Science*, vol. 232, issue 22, 2018.
6. J. Wang, H. Huang, S. Zhang, F. Qin, Z. Wang, T. Liang and H. Zhao. **Development and analysis of a stick-slip rotary piezoelectric positioner achieving high velocity with compact structure**, *Mechanical system and Signal Processing*, vol. 145, 2020.
7. T. W. Na, D. H. Kang, J. Y. Jung, J. H. Han and I. K. Oh. **Linear-to-rotary motion converter using asymmetric compliant mechanics and single-crystal PMN-PT stack actuator,** *Journal of Intelligent Material Systems and Structures* , vol. 25(18), pp. 2221–2227, 2014.
8. R. Wang, X. Zhou, Z. Zhu and Q. Liu. **Compliant linear-rotation motion transduction element based on novel spatial helical flexure hinge**, *Mechanism and Machine Theory*, vol. 92, pp. 330–337, 2015.
9. U. Kothari, V. Awasare, T. Londhe, S. Gofane, S. B. Solepatil, S. P Deshmukh. **Design and Development of Linear and Rotary Flexural Mechanism**, *International Conference on Ideas, Impact and Innovation in Mechanical Engineering*, 2017.
10. S. Pardeshia, S. Kandharkarb and B. Deshmukh, **Monolithic compliant slider crank mechanism for motion amplification**, *5th International Conference of Materials Processing and Characterization*, 2016.
11. A. Gupta, S. S. Rattan and Sudipto Mukherjee. **Dynamic analysis of compliant-based slider crank mechanism using the enviroments like ANSYS**, *International Journal of Mechanisms and Robotic Systems*, vol. 3, no. 4, pp. 317 – 332, 2016.
12. T. P. Dao and S. C. Huang. **Design and Analysis of Flexible Slider Crank Mechanism**, *International Journal of Aerospace and Mechanical Engineering*, vol. 8, no. 5, 2014.
13. R. S. Chiorean, M. C. Dudescu, M. Pustan and M. Hardau. **Analytical and numerical study on the maximum force developed by a V-beam thermal actuator**, *Procedia Technology*, vol. 12, pp. 359-363, 2014.
14. A. S. Joshi, H. Mohammed and S. M. Kulkarni. **Analysis of a chevron beam thermal actuator**, *IOP Conference Series: Materials Science and Engineering*, vol. 310, 2018.
15. N. D. K. Tran, T. G. Nguyen and T. L. Tran. **Optimize design the compliant bistable mechanism based on NSGA-II**, *International Journal of Advanced Trends in Comuter Science and Engineering*, vol. 9, no. 4, 2020.
16. A. Baracu, R. Voicu, R. Müller, A. Avram, M. Pustan, R. Chiorean, C. Birleanu and C. Dudescu. **Design and fabrication of a MEMS chevron-type thermal actuator**, *AIP Conference Proceedings*, vol. 25, 2015.
17. J. Varona, M. T. Torres and A. A. Hamoui. **Design of MEMS vertical–horizontal chevron thermal actuators**, *Sensors and Actuators A: Physical*, vol. 153, pp. 127-130, 2009.
18. E. Rawashdeh, A. Karam and I. G. Foulds. **Characterization of Kink Actuators as Compared to Traditional Chevron Shaped Bent-Beam Electrothermal Actuators**, *Micromachines*, vol. 3, pp. 542-549, 2012.